Vanadium Hydrotris(pyrazolyl)borate Complexes of Diphenyl Phosphate. Heterometallic Complexes of the $[LV\{(PhO)_2PO_2\}_3]^-$ Fragment

Norman S. Dean,[†] Ladd M. Mokry,[†] Marcus R. Bond,[†,‡] Madan Mohan,[†] Tom Otieno,[†,§] C. J. O'Connor,[∥] K. Spartalian,[⊥] and Carl J. Carrano*[,†]

Departments of Chemistry, Southwest Texas State University, San Marcos, Texas 78666, University of New Orleans, New Orleans, Louisiana 70148, and Department of Physics, University of Vermont, Burlington, Vermont 05405

Received August 14, 1996[⊗]

The synthesis and characterization of nine trinuclear, mixed metal complexes of the type $[LV\{\mu\text{-}(PhO)_2PO_2\}_3]_2M$, where the vanadium is in the 3+ oxidation state, L = hydrotris(pyrazolyl)borate, and M = Ba(II) (**1**), Ca(II) (**2**), Mg(II) (**3**), Mn(II) (**4**), Co(II) (**5**), Ni(II) (**6**), Fe(II) (**7**), 2 Na(I) (**8**), Al(III) (**9**), and La(III) (**10**), are described. X-ray crystal structural analysis of **1**, **3**, and **4** gave the following parameters: **1**, $C_{92}H_{84}B_2N_{12}O_{24}P_6Cl_4BaV_2$, $C2/c$, $a = 26.730(5)$ Å, $b = 15.521(3)$ Å, $c = 27.648(6)$ Å, $\beta = 100.53(3)°$, $Z = 4$; **3**, $C_{94}H_{80}B_2N_{14}O_{24}P_6MgV_2$, $P\bar{1}$, $a = 13.410(3)$ Å, $b = 14.179(3)$ Å, $c = 15.694(3)$ Å, $\alpha = 112.22(3)°$, $\beta = 101.31(3)°$, $\gamma = 106.15(3)°$, $Z = 1$; **4**, $C_{111}H_{80}B_2N_{12}O_{28}P_6MnV_2$, $R\bar{3}c$, $a = 18.670(3)$ Å, $b = 18.671(3)$ Å, $c = 61.114(12)$ Å, $Z = 6$. Magnetic measurements indicate that compounds containing an integral spin central ion display moderate antiferromagnetic coupling while those with half-integral spins give more complex behavior.

Introduction

The synthesis of new solid-state vanadium phosphate systems has attracted increasing attention due to their range of applications as size selective inorganic hosts, ion exchangers, and catalyst supports.[1,2] Using hydrothermal synthetic techniques, Zubieta and others have characterized a variety of anionic clusters and layered oxo−vanadium organophosphates.[3−5] While hydrothermal techniques have provided a wealth of materials relevant to the solid-state applications of vanadium phosphates, these complexes arise from a complex and incompletely understood chemistry. In order to provide a more predictable approach to new solid-state materials, we have begun an investigation into the synthesis, through traditional techniques, of discrete vanadium−phosphate complexes which we hope can be precursors to rationally synthesized, extended solid-state materials. Recently we communicated some of the initial results of this study, showing that the product nuclearity was a function of the denticity of both the phosphate and the ancillary ligands employed.[6,7] The $[LV\{\mu\text{-}(PhO)_2PO_2\}_3]^-$ fragment was observed in the linear trinuclear homometallic species $[LV\{\mu\text{-}(PhO)_2PO_2\}_3]_2V^+$, where it acts as a tridentate, facially coordinating three oxygen donor to the central V^{3+} ion.[7] In this regard its behavior is similar to that of the tripodal $[Cp\text{-}M(P(R_2)O)_3]^-$ (M = Co, Rh) complexes of Kläui.[8,9] As the Kläui ligand is capable of forming complexes with a variety of metal ions in the +2 and +3 oxidation states, we decided to explore in more detail the coordination behavior of the $[LV\text{-}\{\mu\text{-}(PhO)_2PO_2\}_3]^-$ fragment and assess its utility as a synthon. In addition to its potential as a chelating agent for M^+, M^{2+}, and M^{3+} ions, these linear trinuclear complexes may display potentially interesting magnetic properties of use in the design of new molecular magnetic materials.

Experimental Section

Materials. All synthetic procedures were carried out under an atmosphere of pure dry argon or nitrogen by utilizing standard Schlenk techniques. Subsequent workup was carried out in air unless otherwise noted. Solvents were distilled under nitrogen from the appropriate drying agents (CaH_2 or Na/benzophenone). DMF was Burdick and Jackson "distilled in glass" grade and was used as received and kept stored under nitrogen. All other materials were reagent grade and used as received. Potassium hydrotris(pyrazolyl)borate was synthesized according to the reported method,[10] as was $[HB(pz)_3]VCl_2\cdot DMF$.[11]

Synthesis. $[LV\{\mu\text{-}(PhO)_2PO_2\}_3]_2Ba$ (1). $[HB(pz)_3]VCl_2\cdot DMF$ (0.814 g, 2.0 mmol) and $Na[(C_6H_5O)_2PO_2]$ (1.608 g, 6.0 mmol) were mixed in a Schlenk flask. CH_3CN (30 mL) was added and the mixture brought rapidly to reflux temperature. The reaction mixture was allowed to stir for 10−15 min producing a clear green solution. $BaCl_2\cdot 2H_2O$ (0.244g, 1.0 mmol) was added to the reaction flask, and the flask was heated until refluxing again. On cooling, a pale green precipitate formed. The precipitate was collected, and the desired product was separated from NaCl formed in the reaction by extraction with warm CH_2Cl_2. Cooling and slow evaporation of the dichloromethane solution produced crystals suitable for a structure determination. Yield: 1.4 g (63%). Anal. Calcd for **1**: C, 50.04; H, 3.73; N, 7.78. Found: C, 50.40; H, 3.71; N, 7.82. IR (cm^{-1}): 2488, 1591, 1490, 1407, 1270, 1204, 1086, 929, 760, 689, 535. UV/vis [λ (ϵ)]: 410 (91), 582 nm

[†] Southwest Texas State University.
[‡] Present address: Department of Chemistry, Southeast Missouri State University, Cape Girardeau, MO 63701.
[§] Present address: Department of Chemistry, Eastern Kentucky University, Richmond, KY 40475.
[∥] University of New Orleans.
[⊥] University of Vermont.
[⊗] Abstract published in *Advance ACS Abstracts,* March 1, 1997.

(1) Johnson, D. C.; Jacobson, A. J.; Butler, W. M.; Rosenthal, S. E.; Brody, J. F Lewandowski, J. T. *J. Am. Chem. Soc.* **1989**, *111*, 381.
(2) Centi, G.; Trifiro, F.; Edner, J. R.; Francetti, V. M. *Chem. Rev.* **1988**, *88*, 55.
(3) Khan, M. I., Zubieta, J. *Progress in Inorganic Chemistry*; John Wiley and Sons, Inc.: New York, 1990; pp 1−150.
(4) Soghomonian, V.; Haushalter, R. C.; Chen, Q.; Zubieta, J. *Inorg. Chem.* **1994**, *33*, 700.
(5) Chen, Q.; Zubieta, J. *Angew. Chem., Int. Ed. Engl.* **1993**, *32*, 261.
(6) Bond, M. R.; Mokry, L. M.; Otieno, T.;Thompson, J.; Carrano, C. J. *Inorg. Chem.* **1995**, *34*, 11894.
(7) Dean, N. S.; Mokry, L. M.; Bond, M. R.; O'Connor, C. J.; Carrano, C. J. *Inorg. Chem.* **1996**, *35*, 3541.
(8) Klaui, W.; Muller, A.; Eberspach, W.; Boese, R.; Goldberg, I. *J. Am. Chem. Soc.* **1987**, *109*, 164.
(9) Shinar, H.; Navon, G.; Klaui, W. *J. Am. Chem. Soc.* **1986**, *108*, 5005.
(10) Trofimenko, S., *J. Am. Chem. Soc.* **1967**, *89*, 3170.
(11) Mohan, M.; Holmes, S. M.; Butcher, R. J.; Jasinski, J. P.; Carrano, C. J. *Inorg. Chem.* **1992**, *31*, 2029.

S0020-1669(96)00979-2 CCC: $14.00

Table 1. Crystallographic Data and Data Collection Parameters for **1**, **3**, and **4**

param	**1**	**3**	**4**
formula	$C_{92}H_{84}B_2N_{12}O_{24}BaP_6Cl_4V_2$	$C_{94}H_{80}B_2MgN_{14}O_{24}P_6V_2$	$C_{111}H_{80}B_2MnN_{12}O_{28}P_6V_2$
space group	*C*2/*c*	*P*$\bar{1}$	*R*3*c*
temp, K	298	298	298
a, Å	26.30(5)	13.410(3)	18.67(3)
b, Å	15.521(3)	14.179(3)	18.671(3)
c, Å	27.648(6)	15.694(3)	61.114(12)
α, deg		112.22(3)	
β, deg	106.49(3)	101.31(3)	
γ, deg		106.15(3)	
V, Å^3	10 999(4)	2496.5(9)	18 455(6)
ρ_{calc}, g cm^{-3}	1.407	1.412	1.258
Z	4	1	6
fw	2330.2	2123.4	2330.1
μ, cm^{-1}	0.078	0.037	0.0398
radiation		graphite-monochromated Mo Kα (0.710 73)	
R,[a] %	5.94	5.89	5.46
R_w,[b] %	7.15	8.20	6.49

[a] Quantity minimized $\omega w(F_o - F_c)^2$, $R = \sum|F_o - F_c|/wF_o$. [b] $R_w = (\omega w(F_o - F_c)^2/\sum(wF_o)^2)^{1/2}$.

(32). The analogous Ca(II) (**2**), Mg(II) (**3**) Mn(II) (**4**), Co(II) (**5**), Ni(II) (**6**), and Fe(II) (**7**) complexes where all obtained in a similar manner starting with the appropriate metal sulfate or chloride salt. Satisfactory analytical data were obtained on all compounds.

[LV{(PhO)$_2$PO$_2$}$_3$]$_2$Na$_2$ (8). [HB(pz)$_3$]VCl$_2$·DMF (0.814 g, 2.0 mmol) and Na[(C$_6$H$_5$O)$_2$PO$_2$] (1.608 g, 6.0 mmol) were mixed in a Schlenk flask. CH$_3$CN (30 mL) was added and the mixture brought rapidly to reflux temperature. The reaction mixture was allowed to stir for 10−15 min producing a clear green solution. The reaction was heated to reflux a second time, allowed to cool, and then filtered to remove NaCl formed in the reaction. The filtrate volume was reduced under a flow of dry N_2, and the product was obtained as a light green crystalline solid. Yield: 1.47 g (70%). Anal. Calcd for **8**: C, 52.25; H, 3.90; N, 8.12. Found: C 52.16; H 3.94; N 7.97. IR (cm^{-1}): 2488, 1588, 1488, 1405, 1283, 1205, 1094, 927, 772, 694, 533. UV/vis [λ (ϵ)]: 414 (43), 596 nm (15).

([LV{(PhO)$_2$PO$_2$}$_3$]$_2$Al)ClO$_4$ (9). [HB(pz)$_3$]VCl$_2$·DMF (0.406 g, 1.0 mmol) was dissolved in MeCN (50 mL)/H$_2$O (5 mL) in a Schlenk flask. Na[(PhO)$_2$PO$_2$] (0.804 g, 3.0 mmol) was added and the reaction allowed to stir for 15−20 min whereupon Al(ClO$_4$)$_3$·9H$_2$O (0.243 g, 0.5 mmol) was added. A light gray/green precipitate formed nearly instantly. The precipitate was filtered off and recrystallized from hot acetonitrile. Yield: 0.144 g (28%). Anal. Calcd for **9**·NaClO$_4$: C, 47.58; H, 3.55; N, 7.40. Found: C, 47.32; H, 3.68; N, 7.48. IR (cm^{-1}): 2491, 1591, 1480, 1407, 1310, 1244, 1203, 1096, 961, 775, 689. UV/vis [λ (ϵ)]: 572 (27), 714 nm (13). The corresponding La(III) complex, **10**, was also prepared, albeit in very low yield, employing a similar method. However, in this case the precipitate was largely insoluble in common solvents and consisted primarily of an insoluble lanthanum phosphate. The desired complex was extracted with dichloromethane and recrystallized from toluene. The IR of the product was essentially identical to that of the Al analog.

Physical Methods. Preliminary determination of magnetic susceptibilities were made at room temperature using a Johnson-Mathey magnetic susceptibility balance, while variable-temperature measurements were performed as previously described over the range of 2−300 K by employing either a SQUID or vibrating sample magnetometer.[12,13] UV/vis spectra were recorded on an HP8452A diode array spectrophotometer. Elemental analysis were performed by Desert Analytical Services.

X-ray Crystallography. Crystals of **1**, **3**, and **4** were sealed in Lindeman glass capillaries and mounted on a Siemens P4 diffractometer. Unit cell constants were determined by least-squares refinement of the angular settings of 12−30 well-centered high-angle reflections. Structure solution and refinement were achieved using the SHELXTL-PLUS crystallography software from Siemens.[14] Pertinent parameters regarding crystal data, data collection, and structure solution and refinement are given in Table 1 for each compound. A structure for the Ca complex, **2**, has also been completed. However as it is not as good as those for **1**, **3**, and **4** and reveals no novel features, it has been relegated to the Supporting Information. Details of the individual structure refinements are summarized below.

[LV{*μ*-(PhO)$_2$PO$_2$}$_3$]$_2$Ba·CH$_2$Cl$_2$ (1). Suitable crystals of **1** were grown by slow evaporation at room temperature of a dichloromethane solution. Structure solution was achieved *via* the Patterson method, with all of the non-hydrogen atoms of the trinuclear unit found from the solution. Several peaks in the difference map were interpreted as a dichloromethane molecule disordered over two sites with occupancies of roughly 0.7 and 0.3, respectively. Anisotropic thermal parameters were refined for all non-hydrogen atoms. Positions of the hydrogen atoms were calculated to give an idealized geometry and then fixed to ride on their respective bound atoms. Final refinement of 674 least-squares parameters against 4744 observed reflections ($F > 4.0\sigma(F)$) gave agreement factors $R = 0.0594$ and $R_w = 0.0715$. The largest peak on the difference map was 0.63 e Å^{-3} while the largest hole was −0.52 e Å^{-3}. Atomic coordinates are listed in Table 2 with pertinent bond distances and angles listed in Table 3.

[HB(pz)$_3$V((C$_6$H$_5$O)$_2$PO$_2$)$_3$]$_2$Mg·2MeCN (3). X-ray-quality crystals of **3** were grown by slow evaporation of an acetonitrile solution of the complex. Structure solution was achieved via direct methods and subsequent structure refinement proceeded normally. Anisotropic thermal parameters were refined for all non-hydrogen atoms. Positions of the hydrogen atoms were calculated to give an idealized geometry and then fixed to ride on their respective bound atoms except for the position of the hydrogen bound to boron, which was located on the difference map and fixed through the remaining cycles of refinement. A fixed isotropic thermal parameter (0.08 Å^2) was assigned to each hydrogen. Final refinement of 646 least-squares parameters against 4299 unique, observed ($F > 4\sigma(F)$) reflections gave agreement factors $R = 0.0589$ and $R_w = 0.0820$ and excursions on the difference map between −0.43 and 0.44 e$^-$/Å^3. Atomic coordinates are listed in Table 4 with selected bond lengths and angles again listed in Table 3.

[HB(pz)$_3$V((C$_6$H$_5$O)$_2$PO$_2$)$_3$]$_2$Mn·3C$_7$H$_8$ (4). Crystals for X-ray analysis were obtained by layering a toluene solution of **4** with hexane and allowing the solution to stand at room temperature for 2 days. Structure solution was achieved *via* the Patterson method with all non-hydrogen atoms of the core found in the initial solution. Several peaks were found on or about a 2-fold rotation axis and isolated from the trinuclear complex. These were interpreted as a 2-fold disordered toluene of crystallization, and the atoms were included in the refinement. Anisotropic thermal parameters were refined for all non-hydrogen atoms. Positions of the hydrogen atoms were calculated to give an idealized geometry and then fixed to ride on their respective bound

(12) O'Connor, C. J. *Prog. Inorg. Chem*. **1982**, *29*, 203.
(13) Mohan, M.; Bond, M. R.; Otieno, T.; Carrano, C. J. *Inorg. Chem*. **1995**, *34*, 1233.
(14) Sheldrick, G. M. SHELXTL-PC, Version 4.1, Siemens X-Ray Analytical Instruments, Inc., Madison, WI, 1989. Scattering factors were from: *International Tables for X-Ray Crystallography*; Ibers, J., Hamilton, W., Eds.; Kynoch: Birmingham, U.K., 1974; Vol. IV.

Table 2. Atomic Coordinates ($\times 10^4$) and Equivalent Isotropic Displacement Coefficients ($Å^2 \times 10^3$) for **1**

	x	*y*	*z*	*U*(eq)[a]
Ba	0	0	0	46(1)
V(1)	1311(1)	−1561(1)	1496(1)	41(1)
P(1)	1479(1)	−135(1)	609(1)	43(1)
P(2)	418(1)	−2318(1)	488(1)	48(1)
P(3)	320(1)	−265(1)	1482(1)	44(1)
O(1)	1465(2)	−855(3)	961(2)	56(2)
O(2)	1012(2)	73(3)	199(2)	52(2)
O(3)	1919(2)	−332(4)	348(2)	59(2)
O(4)	1683(2)	667(3)	967(2)	53(2)
O(5)	758(2)	−2216(3)	1013(2)	58(2)
O(6)	59(2)	−1619(3)	264(2)	57(2)
O(7)	132(2)	−3225(3)	449(2)	65(2)
O(8)	810(2)	−2533(3)	158(2)	55(2)
O(9)	830(2)	−725(3)	1644(2)	57(2)
O(10)	156(2)	121(3)	978(2)	52(2)
O(11)	−88(2)	−938(3)	1579(2)	50(2)
O(12)	315(2)	422(4)	1906(20	52(2)
B(1)	2189(4)	−2503(7)	2369(4)	56(4)
N(1)	1217(3)	−2368(5)	2061(3)	54(3)
N(2)	1637(3)	−2725(5)	2399(3)	61(3)
C(1)	803(4)	−2637(6)	2174(3)	70(4)
C(2)	953(5)	−3182(8)	2595(4)	103(5)
C(3)	1478(5)	−3215(7)	2723(4)	92(5)
N(3)	1886(3)	−2435(4)	1431(2)	47(3)
N(4)	2231(3)	−2756(4)	1853(3)	51(3)
C(4)	2030(4)	−2719(6)	1043(4)	66(4)
C(5)	2470(4)	−3239(7)	1200(4)	83(4)
C(6)	2582(4)	−3237(5)	1707(4)	67(4)
N(5)	1925(2)	−996(4)	2063(2)	46(3)
N(6)	2252(3)	−1516(5)	2415(3)	54(3)
C(7)	2080(3)	−188(6)	2164(3)	57(3)
C(8)	2504(4)	−174(6)	2575(4)	74(4)
C(9)	2607(3)	−1008(7)	2732(3)	65(4)
C(11)	2411(3)	−705(6)	580(4)	59(4)
C(12)	2649(4)	−1101(8)	273(4)	101(5)
C(13)	3117(5)	−1474(9)	464(6)	126(6)
C(14)	3367(5)	−1431(9)	953(6)	112(5)
C(15)	3147(4)	−1041(8)	1274(5)	93(5)
C(16)	2655(4)	−659(7)	1077(4)	73(4)
C(21)	1799(4)	1459(6)	795(4)	63(4)
C(22)	1431(5)	1988(7)	518(5)	109(5)
C(23)	1571(7)	2800(8)	381(6)	175(6)
C(24)	2069(7)	3035(10)	521(7)	169(7)
C(25)	2425(7)	2544(11)	818(8)	213(7)
C(26)	2282(5)	1737(8)	961(6)	150(6)
C(31)	−288(3)	−3414(6)	647(3)	56(3)
C(32)	−473(4)	−4223(7)	560(4)	88(4)
C(33)	−902(6)	−4454(8)	727(5)	122(6)
C(34)	−1109(5)	−3876(10)	982(5)	121(6)
C(35)	−923(5)	−3073(8)	1056(4)	100(5)
C(36)	−505(4)	−2840(7)	896(4)	76(4)
C(41)	634(3)	−2510(6)	−365(3)	52(3)
C(42)	329(4)	−3171(7)	−622(4)	76(4)
C(43)	169(4)	−3140(9)	−1146(4)	95(5)
C(44)	309(5)	−2486(9)	−1394(4)	91(5)
C(45)	610(5)	−1831(7)	−1133(4)	84(4)
C(46)	769(4)	−1842(6)	−621(4)	69(4)
C(51)	−616(3)	−737(5)	1511(3)	50(3)
C(52)	−796(4)	−736(6)	1919(3)	67(4)
C(53)	−1320(4)	−609(7)	1852(5)	88(5)
C(54)	−1662(4)	−485(8)	1395(5)	92(5)
C(55)	−1480(4)	−463(7)	992(4)	84(4)
C(56)	−955(4)	−626(6)	1035(4)	70(4)
C(61)	651(3)	1129(5)	2035(3)	49(3)
C(62)	719(3)	1454(6)	2512(3)	64(4)
C(63)	1028(4)	2177(7)	2649(4)	81(4)
C(64)	1257(4)	2555(7)	2329(5)	88(5)
C(65)	1194(4)	2220(7)	1859(4)	82(4)
C(66)	897(3)	1484(6)	1704(3)	64(4)
C(101)[b]	1138(9)	5525(7)	1215(5)	277(7)
Cl(2)[b]	1240(8)	5062(8)	735(5)	419(7)
Cl(3)[b]	1047(3)	4923(5)	1652(3)	220(5)
C(103)[b]	4946(16)	9126(23)	2445(19)	254(9)
Cl(4)[b]	4652(10)	9802(12)	2023(6)	192(7)
Cl(5)[b]	5516(9)	9426(15)	2767(11)	245(8)

[a] Equivalent isotropic *U* defined as one-third of the trace of the orthogonalized $\mathbf{U}_{ij}$ tensor. [b] Site occupation for C(101), Cl(2), and Cl(3) is 0.705(5) and for C(103), Cl(4), and Cl(5) is 0.295(5).

Table 3. Selected Bond Lengths (Å) and Angles (deg)

	1 (Ba)	**2** (Ca)	**3** (Mg)	**4** (Mn)
$M-O_{mean}$	2.613(8)	2.316(20)	2.074(19)	2.203(6)
$V-O_{mean}$	1.965(9)	1.972(14)	1.975(18)	1.953(6)
$V-N_{mean}$	2.093(13)	2.084(14)	2.104(6)	2.114(9)
$O-M-O_{cis}$ (largest)	101.5(2)	94.0(5)	91.4(2)	95.4(2)
$O-M-O_{cis}$ (smallest)	78.5(2)	86.0(5)	88.6(2)	87.2(2)
max deviation from ideality	11.5°	4°	1.4°	5.4°
$O-M-O_{trans}$	180.0(0)	180.0(0)	180.0(0)	174.2(3)

atoms. A fixed, isotropic thermal parameter was assigned to each hydrogen (0.08 $Å^3$). Hydrogen atom positions were not calculated for the cocrystallized toluene. Final refinement of 248 least-squares parameters against 1077 unique, observed ($F > 6\sigma(F)$) reflections gave agreement factors $R = 0.0546$ and $R_w = 0.0649$ and peaks on the difference map between −0.22 and 0.30 $e^-/Å^3$. Atomic coordinates are listed in Table 5 with bond lengths and angles summarized in Table 3.

Results

Syntheses. Complex **3**, the Mg^{2+}-containing trinuclear species, was initially synthesized as an unexpected product from the reaction of the dinuclear V(III) complex $L_2V_2(\mu\text{-}O)(\mu\text{-}OAc)_2$ with diphenyl phosphoric acid, intended to produce $L_2V_2(\mu\text{-}O)(\mu\text{-}(RO)_2PO_2)_2$. The magnesium ions are apparently being provided by the $MgSO_4$ used as a drying agent during the reaction. Since the analogous Ca complex also originally arose from filtration of the above reaction mixtures through Celite, it became clear that a chelating agent with high affinity for divalent cations must be produced. A rational synthesis was then developed for complex **1**, the trinuclear Ba^{2+} species, which involved heating a mixture of $LVCl_2(DMF)$ and $Na[(PhO)_2PO_2]$ directly in pure MeCN to produce a solution containing the mononuclear fragment $LV((PhO)_2PO_2)_3^-$, which can be isolated as the sodium salt, **8**, the structure of which as been determined.[15] Introduction of the barium ion as a $BaCl_2$ leads to the ready formation of the desired trinuclear species. This synthetic technique proved adaptable to a wide variety of metal chloride or sulfate salts and has been used to produce the trimers species containing Mg^{2+}, Mn^{2+}, Ca^{2+}, Co^{2+}, Fe^{2+}, and Ni^{2+} in the central position. Nitrate salts of these metals are not suitable starting materials, however, since the oxidizing nature of this anion invariably leads only to the isolation of the phosphate-bridged V(IV) dimers previously reported.[16]

Descriptions of Structures. Figure 1 shows the coordination geometry and atom-labeling scheme for **1**. Since the structures of **3** and **4** are nearly identical, figures depicting these species are deposited in the Supporting Information. All of these neutral, linear trimetallic species consist of a central, octahedral divalent metal cation (Ba, Mg, or Mn) facially coordinated on either side by a $LV^{III}((C_6H_5O)_2PO_2)_3^-$ moiety. Each diphenyl phosphate group is monodentate to V(III) leaving one phosphate oxygen free to coordinate the central M^{2+} ion. Thus the central metal is coordinated by six phosphate oxygens with nearly octahedral geometry. As expected the largest deviations from ideal geometry arise with the largest central atom. This is a

(15) The structure of **8** is not up to normal crystallographic standards; hence, we do not report it in full here. However, the atom connectivities are clear even at the present state of refinement: $a = 12.050(4)$ Å, $b = 14.145(5)$ Å, $c = 16.724(4)$ Å, $\alpha = 104.47(3)°$, $\beta = 97.36(2)°$, $\gamma = 114.17(3)°$, $V = 2430.9(14)$ $Å^3$, $Z = 1$, 5573 reflections, 5088 unique ($R_{merg} = 0.076$), 2258 observed ($F > 4\sigma F$), $R =$ ca. 24%. The structure of **8** is similar to that of **1** except that two monovalent Na atoms occupy the central position, bound in distorted tetrahedral geometry to two terminal and two bridging diphenyl phosphate oxygens. The Na···Na distance is 3.16 Å.

(16) Bond, M. R.; Mokry, L. M.; Otieno, T.; Thompson, J.; Carrano, C. J. *Inorg. Chem.* **1995**, *34*, 11894.

Table 4. Atomic Coordinates ($\times 10^4$) and Equivalent Isotropic Displacement Coefficients ($Å^2 \times 10^3$) for **3**

	x	*y*	*z*	*U*(eq)[a]
Mg	5000	5000	5000	23(2)
V(1)	3617(1)	6305(1)	7587(1)	29(1)
P(1)	2725(2)	5552(2)	5247(1)	32(1)
P(2)	4111(2)	4092(2)	6564(1)	31(1)
P(3)	5975(2)	7151(2)	7225(1)	31(1)
O(1)	3122(4)	6292(4)	6325(3)	35(3)
O(2)	3447(3)	5097(4)	4815(3)	36(3)
O(3)	2279(4)	6191(5)	4724(4)	52(3)
O(4)	1605(4)	4642(4)	5057(3)	41(3)
O(5)	3439(4)	4722(4)	6951(3)	35(3)
O(6)	4714(4)	4329(4)	5944(3)	37(3)
O(7)	4910(4)	4197(4)	7521(3)	39(3)
O(8)	3317(4)	2815(4)	5953(3)	43(3)
O(9)	5184(3)	6785(4)	7697(3)	35(2)
O(10)	5705(4)	6548(4)	6163(3)	33(2)
O(11)	6155(4)	8405(4)	7572(3)	38(3)
O(12)	7128(3)	7171(4)	7723(3)	40(3)
B(1)	2793(8)	7423(8)	9370(7)	47(5)
N(1)	2033(5)	5833(5)	7680(4)	41(3)
N(2)	1828(5)	6424(5)	8496(5)	44(4)
C(11)	1068(6)	5002(7)	7049(6)	50(5)
C(12)	254(7)	5073(8)	7452(7)	62(5)
C(13)	759(7)	5956(8)	8360(7)	61(6)
N(3)	3688(5)	7931(5)	8264(4)	38(3)
N(4)	3298(5)	8256(6)	9020(4)	42(4)
C(14)	4037(6)	8791(7)	8088(6)	46(5)
C(15)	3882(7)	9685(8)	8736(7)	55(5)
C(16)	3411(8)	9301(8)	9291(7)	61(5)
N(5)	4119(5)	6500(5)	9026(4)	38(3)
N(6)	3675(5)	7008(5)	9692(4)	45(4)
C(17)	4844(7)	6224(7)	9486(6)	49(5)
C(18)	4857(8)	6547(8)	10450(6)	61(6)
C(19)	4136(8)	7026(8)	10534(6)	57(5)
C(21)	2824(8)	7317(8)	5030(6)	48(5)
C(22)	3923(8)	7820(9)	5319(6)	58(6)
C(23)	4396(9)	8953(10)	5618(7)	77(7)
C(24)	3721(11)	9518(10)	5589(9)	92(8)
C(25)	2619(11)	8998(11)	5302(9)	85(8)
C(26)	2137(8)	7888(9)	5019(7)	60(6)
C(31)	915(6)	3640(6)	4224(5)	33(4)
C(32)	−188(6)	3409(7)	3957(6)	55(5)
C(33)	−887(7)	2408(9)	3183(8)	76(6)
C(34)	−536(9)	1645(8)	2710(8)	78(6)
C(35)	593(7)	1905(7)	2978(7)	73(6)
C(36)	1330(7)	2895(7)	3758(6)	54(5)
C(41)	5850(6)	3947(7)	7553(5)	35(4)
C(42)	5793(7)	2924(8)	6988(6)	53(5)
C(43)	6729(9)	2701(9)	7118(7)	72(6)
C(44)	7690(8)	3452(10)	7785(8)	68(7)
C(45)	7760(8)	4497(10)	8358(9)	81(7)
C(46)	6834(7)	4760(8)	8243(7)	62(6)
C(51)	2517(7)	2267(7)	6250(6)	43(4)
C(52)	1442(8)	2099(9)	5851(7)	75(7)
C(53)	641(9)	1454(12)	6056(10)	110(10)
C(54)	898(11)	1001(10)	6635(10)	99(9)
C(55)	1957(11)	1184(10)	7043(9)	95(9)
C(56)	2819(8)	1806(8)	6828(9)	66(6)
C(61)	6883(5)	9161(6)	7363(5)	34(4)
C(62)	7378(8)	10224(7)	8097(6)	58(5)
C(63)	8043(8)	11003(8)	7932(7)	68(6)
C(64)	8217(8)	10766(8)	7082(9)	69(7)
C(65)	7752(8)	9686(8)	6353(7)	65(6)
C(66)	7049(7)	8876(7)	6497(6)	50(5)
C(71)	7751(6)	7706(6)	8716(6)	41(4)
C(72)	8786(7)	7715(9)	8919(7)	75(6)
C(73)	9470(10)	8237(11)	9892(9)	111(9)
C(74)	9099(10)	8720(10)	10626(8)	100(8)
C(75)	8062(10)	8687(8)	10404(7)	83(6)
C(76)	7371(7)	8180(7)	9432(6)	58(5)
N(10)	9706(11)	6437(12)	957(14)	176(11)
C(100)	8872(15)	6253(12)	1062(12)	128(10)
C(101)	7805(12)	5997(11)	1173(10)	116(9)

[a] Equivalent isotropic *U* defined as one-third of the trace of the orthogonalized $\mathbf{U}_{ij}$ tensor.

Table 5. Atomic Coordinates ($\times 10^4$) and Equivalent Isotropic Displacement Coefficients ($Å^2 \times 10^3$) for **4**

	x	*y*	*z*	*U*(eq)[a]
Mn	3333	6667	4167	51(1)
V(1)	3333	6667	3388(1)	49(1)
P(1)	2962(2)	7694(2)	3762(1)	55(1)
O(1)	3349(4)	7549(4)	3563(1)	58(3)
O(2)	2724(4)	7156(4)	3955(1)	60(3)
O(3)	3564(5)	8614(4)	3844(1)	76(4)
O(4)	2186(5)	7705(5)	3656(1)	71(4)
B(1)	3333	6667	2862(3)	63(5)
N(1)	2410(5)	6571(5)	3170(1)	53(4)
N(2)	2512(5)	6589(5)	2950(1)	60(4)
C(11)	1660(7)	6463(6)	3208(2)	67(5)
C(12)	1296(7)	6420(7)	3004(2)	72(5)
C(13)	1851(7)	6493(7)	2849(2)	70(5)
C(21)	4141(8)	9216(7)	3706(2)	68(5)
C(22)	3964(10)	9585(9)	3542(2)	119(6)
C(23)	4574(13)	10197(10)	3413(2)	152(6)
C(24)	5336(13)	10407(9)	3457(3)	150(6)
C(25)	5567(9)	10076(9)	3613(3)	121(6)
C(26)	4959(8)	9446(8)	3744(2)	83(5)
C(31)	1577(7)	7811(7)	3759(2)	65(5)
C(32)	1517(8)	7868(8)	3973(2)	106(6)
C(33)	892(9)	7981(11)	4057(2)	132(6)
C(34)	337(8)	8018(9)	3925(2)	115(6)
C(35)	400(8)	7969(8)	3708(2)	100(6)
C(36)	1024(7)	7864(7)	3622(2)	82(5)
C(51)	109(9)	3333	833	1044(8)
C(52)	206(10)	2778(7)	701(2)	676(7)
C(53)	964(10)	2802(11)	694(3)	800(8)
C(54)	1604(9)	3333	833	1043(8)
C(55)	1053(17)	2188(26)	560(8)	2186(8)

[a] Equivalent isotropic *U* defined as one-third of the trace of the orthogonalized $\mathbf{U}_{ij}$ tensor.

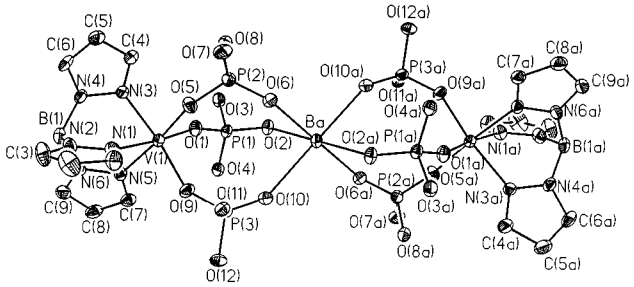

Figure 1. ORTEP diagram (30% probability ellipsoids) with atom-labeling scheme for **1**.

result of the restricted "bite" of the $LV^{III}((C_6H_5O)_2PO_2)_3^-$ moiety. The deviations from ideality range from 12° in **1** to only 0.8° for the V(III) analog which have atomic radii of 1.49 and 0.78 Å, respectively. The two terminal vanadium(III) cations exhibit a trigonally-distorted octahedral coordination with three nitrogens coordinating the terminal face ($[N-V-N]_{mean} = 84.5°$ for **1**, **3**, and **4**) and three oxygen atoms coordinating the bridging face ($[O-V-O]_{mean} = 93.9°$ for **1**, 92.1° for **2**, and 92.8° for **4**).

The site symmetry for the Mg-centered species is formally $\bar{1}$, but approximately trigonal, if phenyl ring conformations are ignored, while the Mn-centered trimer has formal 32 symmetry with the 3-fold axis coincident with the trimer axis in both cases. This (approximate) trigonal symmetry is easily observed from the propeller-like disposition of the pyrazole rings of the terminal capping ligand which radiate out from the trimer axis at a dihedral angle of 120.0 ± 2.5°. Surprisingly, the bridging diphenyl phosphate groups are not coaxial but are twisted slightly relative to the dimer axis as measured by the angle between this axis and the bridging O···O vector. The bridging unit of the trimer can be considered as a polycyclic system, made up of three eight-membered $V(OPO)_2M$ rings similar to

Table 6. NMR Resonances for Linear Trinuclear Complexes (ppm from TMS)

complex	H3	H5	H4	solvent[a]
1 (Ba)	−19.12	−3.00	+10.87	$CDCl_3$
8 (Na)	−19.20	−3.03	+10.79	ACN-d_3
9 (Al)	−20.00	0.00	+10.38	ACN-d_3
V	−20.09	+1.99	+10.21	ACN-d_3

[a] ACN = acetonitrile.

those found in other vanadium diphenyl phosphate aggregates. In compounds **1**, **3**, and **4** the two metal atoms are common to all three rings and a boat conformation is expected since the phosphate groups lie away from the metal−metal axis. However, the twist of the bridging phosphates relative to the trimer axis produces a conformation that is more accurately described as a twisted boat ($[V-O-P]_{mean} = 153.3°$ for **1**, 141.0° for **3**, and 142.0° for **4**).

Paramagnetic NMR. The electronic relaxation properties of V(III) complexes of the type reported here have proved favorable for the observation of relatively sharp paramagnetically shifted NMR spectra. As expected, **1** shows three well-resolved paramagnetically shifted resonances at −19.1, −3.0, and +10.9 ppm assigned as the H3, H5, and H4 protons, respectively, on the tris(pyrazolyl)borate rings (Table 6). The assignments are based on comparison to previously reported (μ-phosphato) vanadium(III) dimers.[17] The observation of only three resonances confirms the 3-fold cylindrical symmetry expected of **1** on the basis its solid-state structure. The NMR spectrum of the sodium salt, **8,** is very similar to that of **1** again indicating 3-fold symmetry although it is unclear that the solid-state structure is maintained in solution. Assuming a simple π delocalization pathway for the unpaired electron density, an alternating sign pattern around the aromatic pyrazolyl ring is expected[18] and indeed observed. However, in the complex with Al(III) as the central metal, **9**, and in the all V(III) complex previously reported there is a reduction in the shift for H5 which moves downfield to 0.0 ppm for the Al and +2.0 ppm for V.

Magnetic Measurements. Susceptibility data for the Ca^{2+}-centered trimer, **2**, show paramagnetic behavior with a gradual decrease in χT with decreasing temperature at the lowest temperatures. Fits of the data to models for simple isotropic exchange-coupling (J), zero-field splitting (D), and g-value were attempted, but all yielded less than satisfactory fits with a high degree of correlation between parameters. An adequate fit was obtained however using a standard spin Hamiltonian for an $S = 1$ system containing both axial and rhombic terms.

$$H = D[S_z - S(S+1)/3] + E(S_x^2 - S_y^2) + 2\beta \mathbf{H}_{app} \cdot \mathbf{g} \cdot \mathbf{S}$$

The first two terms represent respectively the axial and rhombic terms with the last term being the Zeeman interaction in an external field, $\mathbf{H}_{app}$. The adjustable parameters are D, E, and the principal values g_{xx}, g_{yy}, and g_{zz}. The two vanadium sites were assumed to be identical; hence, only a single set of such parameters are needed. For a given orientation of the applied field with respect to the crystalline *xyz*-axis system, the spin Hamiltonian is diagonalized and the projection of the magnetic moment in the field direction is calculated. A polycrystalline average is obtained by stepping the applied field in equal increments of solid angle over an octant of a unit sphere. In the present case a 10 × 10 grid was used. The best fit parameters obtained by least-squares analysis were $D = -36.1$ cm^{-1}, $E = 1.19$ cm^{-1}, $g_{xx} = 1.574$, $g_{yy} = 2.184$, and $g_{zz} = 1.147$ (Figure 2). The spin Hamiltonian parameters calculated using this model are in line with those expected on the basis of other V(III) complexes.[19] The relatively large departure of the principal g components from their usual value near 2 is probably an indication of a significant orbital contribution to the magnetic moment. Construction of a crystal field model, now in progress, should help clarify this point.

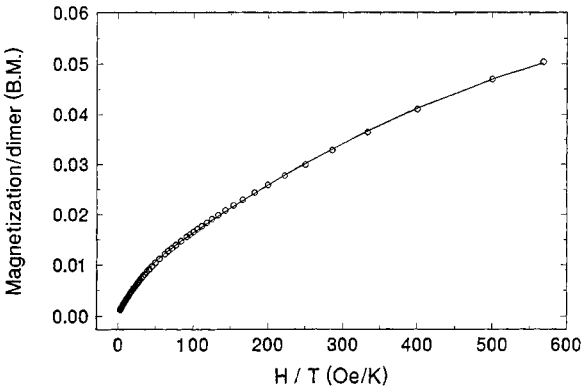

Figure 2. Plot of magnetization per dimer vs H/T for complex **2**. The solid line is the calculation based on the spin Hamiltonian as explained in the text.

The plot of χT versus temperature for the Co^{2+}-centered trimer, **5**, is linear at the highest measured temperatures, so an empirical correction for temperature-independent susceptibility was applied to the data (because of the temperature-variable moment of the Co^{2+} ion, this may not be entirely appropriate). The corrected χT curve has a maximum value of 4.4 (emu K)/mol which gradually decreases to a constant value of 2.5 (emu K)/mol at lowest temperatures. The complicated single-ion magnetic properties of Co^{2+} over the full temperature range have prevented successful fitting of the data to any relatively simple model.

The Fe^{2+}-centered trimer, **7**, exhibits simple paramagnetic behavior close to room temperature with χT a constant 5.1 (emu K)/mol. Decreasing temperature eventually leads to a decrease in χT to 1.3 at the lowest temperature. The data were fit to a simple Heisenberg−Dirac−Van Vleck (HDVV) model with $J = J_{12} = J_{23}$ and $J_{13} = 0$ (where 1 and 3 are the terminal spins and 2 is the central spin). Spin-state energies were as follows: one singlet at $12J$; one triplet each at $6J$ and $10J$; one quintet each at $0J$, $2J$, and $6J$; one septet each at $-4J$ and $0J$; one nonet at $-8J$. Use of these energies and multiplicities in the Van Vleck equation, assuming equivalent g-values at each site, yielded the expression for susceptibility. A least-squares fit of the χT data (Figure 3) to this model yielded reasonable agreement, except at lowest temperature where the model tends toward zero faster than the data, with parameters $J/k = -0.94(2)$ K and $g = 2.054(1)$. The difficulty in the fit at lowest temperature probably arises from the oversimplified assumption of equivalent g-values on the paramagnetic centers. If the g-values are equivalent, then the antiferromagnetic (AFM) alignment of the $S = 1$ V(III) ions with the $S = 2$ Fe(II) ion should lead to $\chi T = 0$ at 0 K. But the g-values of these species almost certainly differ, the g-value of the Fe(II) center being significantly greater than 2.0 and the g-values of the V(III) centers being significantly less than 2.0. This mismatch in g-value would lead to a nonzero value of χT at 0 K, as the trend in data indicates, and a spin alignment that might be

(17) Bond, M. R.; Czernuszewicz, R. S.; Dave, B. C.; Yan, Q.; Mohan, M.; Verastegue, R.; Carrano, C. J. *Inorg. Chem.* **1995**, *34*, 5857.
(18) Swift, T. J. In *NMR of Paramagnetic Molecules; Principles and Applications*, La Mar, G. N., Ed.; Academic Press: New York, 1973.
(19) Carlin, R. L. *Magnetochemistry*; Springer-Verlag: Berlin, 1986.

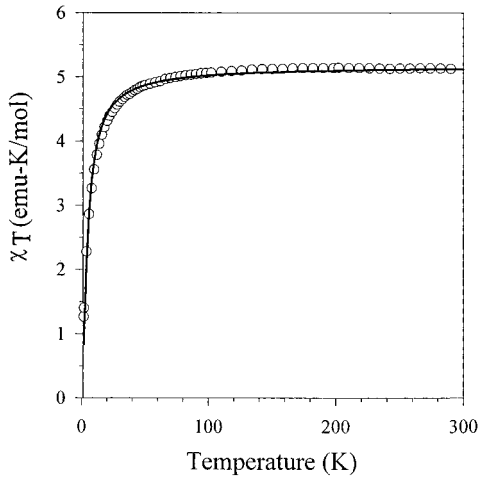

Figure 3. Plot of χT vs T for **7** (open circles) with the fit to the equation described in the text (solid line).

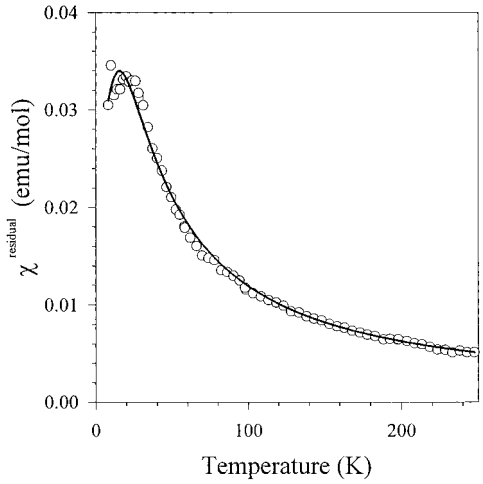

Figure 4. Plot of residual (as described in the text) χT vs T for **4** (open circles) with the fit to the equation described in the text (solid line).

termed, more properly, as ferrimagnetic rather than antiferromagnetic.

The χT data for the Mn(II)-centered trimer show, after an empirical correction for temperature-independent susceptibility, a trend similar to that of the Co^{2+}-centered trimer, i.e. a relatively constant value at high temperature followed by a decrease toward a minimum, but nonzero, value of χT. This decrease occurs over a much narrower temperature range than that of the Co^{2+}-centered trimer (possibly because of the more complicated single-ion properties of the latter). Nevertheless in both cases, the low-temperature χT reaches a value consistent with the values expected for the central ions alone. This implies AFM alignment of the terminal V(III) spins with each other. To analyze the data then, the contribution to χT by the Mn(II) (assuming $g = 2.000$ for Mn(II)) was subtracted from the overall measurement at each temperature and the residual χT divided by T to yield a residual susceptibility. The plot of residual susceptibility versus temperature yields an AFM-like curve with a maximum close to 20 K (Figure 4). A least-squares fit of the residual susceptibility to an $S = 1$ dimer model with ZFS yielded an acceptable fit with $J/k = -6.5(2)$ K, $g = 1.62(8)$, and $D/k = 31(4)$ K (singlet low).

Discussion

The synthesis of tris(pyrazolyl)borate complexes containing phosphate diesters was initially undertaken as part of a study of magneto−structural correlations in $[V_2O]^{4+}$ complexes containing a μ-oxo−bis(μ-acetato) core. As part of a program to synthesize complexes with increasing metal-metal separations, and hence an increasing V−O−V bridging angle, the synthesis of analogous phosphate complexes was investigated. The μ-oxo−bis(μ-acetato) structure is known for a variety of transition metals, most notably iron and manganese, and a procedure for the synthesis of μ-phosphate derivatives from the acetate complexes had been published by Lippard and Armstrong for analogous iron complexes.[20] Following that procedure, the vanadium acetate species was treated with diphenylphosphoric acid in a two-phase CH_2Cl_2/H_2O reaction system. The product of this reaction was however the unexpected linear trinuclear species **3**. The source of the Mg ion in **3** was found to be the anhydrous $MgSO_4$ used as a drying agent in the procedure. Complex **1** can be viewed as a trinuclear heterometallic complex, where it has structural similarities to known linear trinuclear acetate species.[21] A second way of viewing **3** is that of an assembly of two negatively charged $[LV\{(PhO)_2PO_2\}_3]^-$ fragments bound by the doubly charged magnesium ion, suggesting that the synthesis of similar trinuclear complexes containing other M^{2+} ions would be possible. Reaction of $LVCl_2 \cdot DMF$ with 3 equiv of the sodium salt of diphenylphosphoric acid in MeCN produces a solution which reacts cleanly with the alkaline earth chlorides or sulfates to produce the desired Mg-, Ca-, or Ba-containing trinuclear species as sparingly soluble gray/green powders. The complexes are readily dissolved in CH_2Cl_2, which provides a convenient method for both separation of the sodium chloride formed in the reaction from the desired product and crystallization *via* slow evaporation of the solvent. Crystallographically, all of the trinuclear complexes characterized to date have been found to contain solvent molecules in the crystal lattice and better crystallinity has been found in products recrystallized from "wet" CH_2Cl_2 rather than distilled dichloromethane.

Of particular interest to us is the ability to systematically change structural parameters in simple vanadium phosphate systems and to observe the corresponding changes in the interactions between the vanadium ions. Previously we have reported how changing the terminal capping ligand, L, from tris(pyrazolyl)borate to the more sterically demanding tris(3,5-dimethylpyrazolyl)borate[16] causes a significant increase in the vanadium−vanadium separation in the vanadium(IV) complexes of the type $L_2V_2O_2(\mu\text{-}(PhO)_2PO_2)_2$ and how changing from the potentially bidentate diphenyl phosphate to the potentially tridentate monophenyl phosphate results in the isolation of homometallic tetranuclear vanadium(III) species.[22] The ability to place various metal ions into the central position in the trinuclear species provides yet another avenue for controlling a structural property by varying the size of the M^{2+} ion and, hence, the vanadium-to-M^{2+} and vanadium-to-vanadium distances; *i.e.*, moving from the magnesium to the barium species increases the overall distance between the vanadium atoms from ~9.2 to 10.8 Å. It also provides a means to systematically examine magnetic properties.

The magnetic properties for trimers containing integral-spin central ions appear relatively clear. For $S = 0$ (Ca^{2+}), the weak deviations from the uncoupled limit that occur are due to single-ion ZFS rather than exchange coupling between the distant V(III) centers. For $S = 1$ (V^{3+}, previous work) and $S = 2$ (Fe^{2+})

(20) Armstrong, W. H.; Lippard, S. J. *J. Am. Chem. Soc.* **1985**, *107*, 3730.
(21) Kitajima, N.; Amagai, H.; Tamura, N.; Ito, M.; Moro-oka, Y.; Heerwegh, K.; Penicaud, A.; Mathur, R.; Reed, C. A.; Boyd, P. D. *Inorg. Chem.* **1993**, *32*, 3583.
(22) Otieno, T.; Mokry, L. M.; Bond, M. R.; Carrano, C. J.; Dean, N. S. *Inorg. Chem.* **1996**, *35*, 850.

more substantial deviations occur but they can be well-explained in both cases in terms of isotropic AFM coupling between the terminal and central ions. The magnetic behavior of the trimers containing half-integral spin central ions is much more perplexing. Instead of a value of χT at 0 K that would correspond to a simple AFM ground state, these trimers appear to assume, at low temperature, the value of the central ion paramagnetism alone. This would imply that the paramagnetism of the terminal spins is absent, but the mechanism by which this occurs is unclear. In the absence of a paramagnetic central ion (the Ca^{2+}-centered trimer) the terminal V(III) ions show no strong inter- or intratrimer coupling or ZFS effects that might typically be invoked to account for loss of terminal ion paramagnetism. Likewise, the integral-spin trimers show low-temperature susceptibilities that show no apparent effects beyond isotropic exchange coupling. A possible explanation for the low-temperature behavior of the half-integral trimers is the presence of antisymmetric exchange leading to antiparallel alignment of the terminal spins. The antisymmetric exchange Hamiltonian, $\mathbf{d}_{ij}(\mathbf{S}_i \times \mathbf{S}_j)$, results in orthogonal alignment of coupled spins with both spins, then, orthogonal to the coupling vector $\mathbf{d}_{ij}$. The coupling vector would lie parallel to the symmetry axis of the trimer leading to alignment of the spins in the plane perpendicular to the symmetry axis, an alignment that corresponds to the singlet-low state favored by ZFS in V(III). The inversion symmetry of the trimer would require, then, the two coupling vectors between the central ion and the terminal ions to be the same magnitude but opposite directions. This would lead to perpendicular alignment of the terminal spins with the central spin *and antiparallel alignment of the terminal spins with each other*, thus reproducing the observed low-T magnetic behavior. The complexity of this magnetic model along with the futility of fitting isotropic magnetic data to an anisotropic model has prevented a quantitative test of this hypothesis.

Conclusions. A new class of monoanionic, facially coordinating chelating agents based on the $[LV\{(PhO)_2PO_2\}_3]^-$ fragment, which have a high affinity for divalent cations, has been prepared. These linear trimetallic species show interesting magnetic behavior with those complexes containing an integral spin central ion showing straightforward antiferromagnetic coupling while those with half-integral spins showing more complex and as yet incompletely understood behavior.

Acknowledgment. This work was supported by Grant AI-1157 from the Robert A. Welch Foundation, the ACS/PRF, and Grant SF-93-12 from the Dreyfus foundation. The NSF-ILI program Grant USE-9151286 is acknowledged for partial support of the X-ray diffraction facilities at Southwest Texas State University.

Supporting Information Available: Complete lists of atomic positions and *U* values, bond lengths and angles, anisotropic thermal displacement parameters, hydrogen atom coordinates, and data collection and crystal parameters and ORTEP plots showing the atom-labeling schemes for **1**−**4** (41 pages). Ordering information is given on any current masthead page.

IC960979I